Study of Control System Effectiveness in Alleviating Vortex Wake Upsets

Walter A. Johnson* and Gary L. Teper†
Systems Technology, Inc., Hawthorne, Calif.
and
Herman A. Rediess‡
NASA Flight Research Center, Edwards, Calif.

The problem of an airplane being upset by encountering the vortex wake of a large transport on takeoff or landing is currently receiving considerable attention. This paper describes the technique and results of a study to assess the effectiveness of automatic control systems in alleviating vortex wake upsets. A six-degree-of-freedom nonlinear digital simulation was used for this purpose. The analysis included establishing the disturbance input due to penetrating a vortex wake from an arbitrary position and angle. Simulations were computed for both a general aviation airplane and a commercial jet transport. Dynamic responses were obtained for the penetrating aircraft with no augmentation, and with various command augmentation systems. The results of this preliminary study indicate that it is feasible to use an automatic control system to alleviate vortex encounter upsets.

I. Introduction

SEVERAL incidences have occurred in which an airplane has been severely upset by flying into the vortex wake of a large jet transport during landing approach or takeoff. A number of these encounters involving general aviation type aircraft and one involving a transport resulted in fatal crashes.[1] Flight tests reported in Ref. 2 further confirm the inability of a pilot to cope with the severe upsets. To reduce such severity, considerable effort is being spent to predict the wake locations, and to find ways of dissipating the vortices without degrading the performance of the generating aircraft. An alternate approach is to attempt to reduce the response of the penetrating aircraft to an acceptable level by means of an automatic control system.

A brief study was conducted to determine the potential usefulness of command augmentation systems for alleviating vortex wake encounter upsets and to identify those characteristics of the system that are desirable and those that are undesirable. It is emphasized that the study was preliminary and only meant to give a first-order assessment of the feasibility of the approach.

A six-degree-of-freedom, nonlinear digital simulation was used to analyze the dynamic response of the aircraft as it traversed the vortex wake. The study consisted of: establishing the disturbance input due to penetrating a vortex wake; developing a dynamic simulation of an aircraft penetrating a vortex wake from an arbitrary position and angle; computing the responses of two types of aircraft with and without automatic control systems when penetrating the vortex wake from the most critical angles and displacements; and assessing the effectiveness of the various automatic control systems to alleviate vortex wake encounter upsets.

Presented as Paper 73-833 at the AIAA Guidance and Control Conference, Key Biscayne, Fla., August 20–22, 1973; submitted September 10, 1973; revision received January 24, 1974. This research was accomplished for the National Aeronautics and Space Administration under Contract NAS4-1952.

Index categories: Aircraft Flight Operations; Aircraft Handling, Stability, and Control.

*Senior Research Engineer. Member AIAA.

† Principal Specialist. Member AIAA.

‡ Deputy Director, Vehicle Dynamics and Control Division. Member AIAA.

The two example aircraft simulated were a general aviation airplane penetrating the vortex wake of an executive jet transport at separations of 3 and 10 miles, and a commercial jet transport penetrating the vortex wake of a jumbo jet transport at a separation of 3 miles. The types of automatic control systems considered were bank angle command, heading command, and roll rate command. In each case a pitch command system was also used. The simulation did not include pilot control inputs.

This paper describes the simulation used and the preliminary results obtained and indicates the follow-on study effort now underway. Previous studies have considered the effects of a vortex wake on a trailing aircraft. Reference 3 calculated the static moments produced assuming the aircraft was placed at the worst location in the vortex. A complete digital simulation of the dynamic response of an aircraft penetrating a vortex wake was used in Ref. 1; however, it did not assess automatic control systems for possibly alleviating the upset, the primary thrust of this paper.

II. Digital Simulation Description

A general nonlinear six-degree-of-freedom digital simulation for rigid body aircraft dynamics was available at Systems Technology, Inc., for use in this study. Therefore, it was only necessary to implement the desired automatic control systems and to develop a disturbance function due to vortex wake penetration. The latter was accomplished using aerodynamic strip theory and an existing mathematical model for the vortex velocity field, as outlined below.

Vortex Model

The vortex model used, which was taken from Ref. 3, is defined by the tangential flow characteristics given below (axial flow was ignored, giving a two-dimensional flow).

$$|V_T| = \frac{\Gamma_0}{2\pi r}\left[1 - e^{-\left(\frac{r^2}{4\epsilon\tau}\right)}\right]$$

where V_T = the tangential vortex velocity, $\Gamma_0 = 4W_G/\pi\rho V_G b_G$ represents the strength of the vortex (it is a function of the weight, speed, and wing span of the generating airplane), $\epsilon = 0.0002\ \Gamma_0$ represents the vortex decay effect,

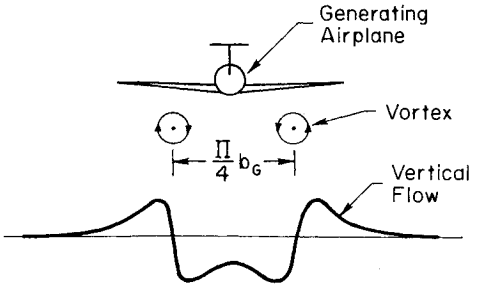

Fig. 1 Sketch of the vortex flowfield.

Table 1 Tangential flow characteristics of a single vortex

Generating airplane	Separation distance	Radius for maximum velocity	Maximum velocity
C-5A	3 mile	19.5 ft	34 fps
Jetstar	3 mile	8.5 ft	17 fps
	10 mile	15.6 ft	9 fps

τ represents the age of the vortex, and r is the radial distance from the center of the vortex.

The centers of the two vortices from the generating airplane are assumed to be straight lines at a constant altitude, parallel to each other at a distance $(\pi/4)b_G$ apart.[3] A sketch of the resulting vertical flow from both vortices is shown in Fig. 1, and some pertinent numerical values for a single vortex are given in Table 1.

Strip Theory

Because the vortices produce a highly nonuniform local flow over the lifting surfaces of the penetrating airplane, strip theory was used to compute the forces and moments caused by the vortex flow (see Ref. 4). To implement this, the penetrating airplane was assumed to have three lifting surfaces: a wing, a horizontal tail, and a vertical tail. Each of these surfaces was divided into chord-wise strips as shown in Fig. 2. The wing was divided into 20 strips per semispan, while the horizontal and vertical tails were each divided into 6 strips per semispan. The distributed forces along the fuselage were modeled via a pitching moment and a yawing moment respectively proportional to the vortex-flow-induced incremental angles of attack and sideslip measured at the wing ¼ root chord.

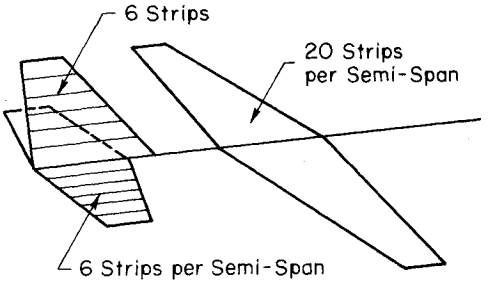

Fig. 2 Strip theory geometry.

Flow at Each Strip

$\bar{w}_{i(E)} \equiv (w_x, w_y, w_z)_E$ is the velocity vector of the wind at any point (i) in space (due to both vortices) expressed in "earth-fixed" axes. From Fig. 3 it can be seen that

$$w_x = 0$$

$$w_y = -w_L\left(\frac{z}{r_L}\right) + w_R\left(\frac{z}{r_R}\right)$$

$$w_z = +w_L\left(\frac{y+s'}{r_L}\right) - w_R\left(\frac{y-s'}{r_R}\right)$$

where w_L and w_R are the tangential flow magnitudes of the left and right vortices, respectively.

Clearly, $\bar{w}_{i(E)}$ is a function of the position of the point in space being considered $(\bar{R}_{i(E)})$; i.e., $\bar{w}_{i(E)} = \bar{w}_{i(E)}(\bar{R}_{i(E)})$. But points of interest for flow calculations will be points on the airplane expressed in airplane body axes. Thus

$$\bar{R}_{i_E} = \bar{R}_{cg_E} + T\bar{R}_{i_B}$$

where $\bar{R}_{cg}$ is the position of the airplane c.g. in earth axes, T is the transformation matrix from airplane body axes to earth axes, and $\bar{R}_{i(B)}$ is the position of a point on the airplane expressed in airplane body axes.

For force calculations we need to know the flow (due to the vortices) in airplane body axes. Thus

$$\bar{w}_{i_B} = T^{-1}\bar{w}_{i_E}$$

Note that:

$$\bar{w}_{i_B} \equiv \begin{pmatrix} u_i \\ v_i \\ w_i \end{pmatrix}_B$$

The incremental angles of attack and sideslip are defined as

$$\Delta\alpha_i \equiv \frac{-w_i}{V}, \quad \Delta\beta_i \equiv \frac{-v_i}{V}$$

Putting all this together gives

$$\begin{pmatrix} 0 \\ \Delta\beta_i \\ \Delta\alpha_i \end{pmatrix}_B = \frac{-1}{V}[T]^{-1}\begin{pmatrix} 0 \\ w_y \\ w_z \end{pmatrix}_E$$

or

$$\begin{pmatrix} 0 \\ \Delta\beta_i \\ \Delta\alpha_i \end{pmatrix}_B = \frac{-\Gamma_0}{2\pi V}[T]^{-1}\begin{bmatrix} 0 \\ \left[\frac{-z}{z^2+(y+s')^2}\right]\left[1-e^{\frac{-z^2-(y+s')^2}{4\epsilon\tau}}\right] + \left[\frac{z}{z^2+(y-s')^2}\right]\left[1-e^{\frac{-z^2-(y-s')^2}{4\epsilon\tau}}\right] \\ \left[\frac{y+s'}{z^2+(y+s')^2}\right]\left[1-e^{\frac{-z^2-(y+s')^2}{4\epsilon\tau}}\right] - \left[\frac{y-s'}{z^2+(y-s')^2}\right]\left[1-e^{\frac{-z^2-(y-s')^2}{4\epsilon\tau}}\right] \end{bmatrix}_E$$

and

$$\begin{pmatrix} x \\ y \\ z \end{pmatrix}_E = \begin{pmatrix} x_{cg} \\ y_{cg} \\ z_{cg} \end{pmatrix} + [T]\begin{pmatrix} x_i \\ y_i \\ z_i \end{pmatrix}_B$$

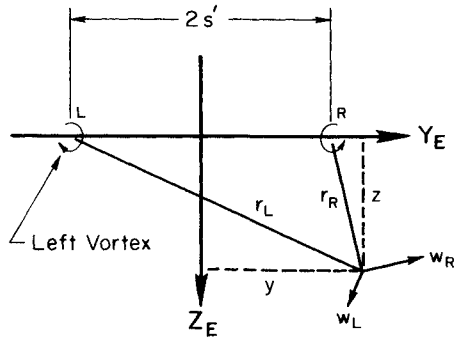

Fig. 3 Flow at an arbitrary point (y, z) due to the left and right vortices of a generating airplane.

Incremental Forces Induced on Each Strip

The incremental force on each strip is assumed to act at the intersection of the 0.25 $\bar{c}$ and the centerline of the strip and is proportional to the incremental angle of attack at the 0.75 $\bar{c}$ of the strip.[4] The incremental forces on each strip are summed as shown below to give the net forces and moments on the airplane. The notation used here is defined as follows:

$W \equiv$ wing
$H \equiv$ horizontal tail
$V \equiv$ vertical tail
$F \equiv$ fuselage
$N_W = 20$
$N_H = N_V = 6$

The subscript "i" is used for the right side of the airplane and for the vertical tail, while "j" is used for the left side of the airplane.

$$\Delta Z_{\text{vortex}} = -\bar{q}\left[C_{L_{\alpha_W}}\left(\sum_{i=1}^{N_W} S_{W_i}\alpha_{W_i} + \sum_{j=1}^{N_W} S_{W_j}\alpha_{W_j}\right) + C_{L_{\alpha_H}}\left(1 - \frac{d\epsilon}{d\alpha}\right)\left(\sum_{i=1}^{N_H} S_{H_i}\alpha_{H_i} + \sum_{j=1}^{N_H} S_{H_j}\alpha_{H_j}\right)\right]$$

$$\Delta Y_{\text{vortex}} = -\bar{q}C_{L_{\alpha_V}}\left(1 - \frac{d\sigma}{d\beta}\right)\sum_{i=1}^{N_V} S_{V_i}\beta_{V_i}$$

$$\Delta L_{\text{vortex}} = \bar{q}\left[-C_{L_{\alpha_W}}\left(\sum_{i=1}^{N_W} S_{W_i}\alpha_{W_i}y_{W_i} + \sum_{j=1}^{N_W} S_{W_j}\alpha_{W_j}y_{W_j}\right)\right.$$
$$-C_{L_{\alpha_H}}\left(1 - \frac{d\epsilon}{d\alpha}\right)\left(\sum_{i=1}^{N_H} S_{H_i}\alpha_{H_i}y_{H_i} + \sum_{j=1}^{N_H} S_{H_j}\alpha_{H_j}y_{H_j}\right)$$
$$\left. + C_{L_{\alpha_V}}\left(1 - \frac{d\sigma}{d\beta}\right)\sum_{i=1}^{N_V} S_{V_i}\beta_{V_i}Z_{V_i}\right]$$

$$\Delta M_{\text{vortex}} = \bar{q}\left[C_{L_{\alpha_W}}\left(\sum_{i=1}^{N_W} S_{W_i}\alpha_{W_i}x_{W_i} + \sum_{j=1}^{N_W} S_{W_j}\alpha_{W_j}x_{W_j}\right) + M_{\alpha_F}\alpha_F + C_{L_{\alpha_H}}\left(1 - \frac{d\epsilon}{d\alpha}\right)\left(\sum_{i=1}^{N_H} S_{H_i}\alpha_{H_i}x_{H_i} + \sum_{j=1}^{N_H} S_{H_j}\alpha_{H_j}x_{H_j}\right)\right]$$

$$\Delta N_{\text{vortex}} = \bar{q}\left[-C_{L_{\alpha_V}}\left(1 - \frac{d\sigma}{d\beta}\right)\sum_{i=1}^{N_V} S_{V_i}\beta_{V_i}x_{V_i} + N_{\beta_F}\beta_F\right]$$

α_F and β_F are evaluated at the 0.25 $\bar{c}$ of the wing root chord.

Table 2 Parameters used for matching strip theory results to known vehicle characteristics

Known vehicle characteristics	Strip theory parameters to be adjusted
Z_w	$C_{L_{\alpha_W}}$
M_w	$C_{L_{\alpha_H}}$, $(d\epsilon/d\alpha)$, M_{α_F}
N_β	$C_{L_{\alpha_V}}$, $(d\sigma/d\beta)$, N_{β_F}
L_p	$C_{L_{\alpha_W}}$ as $f(y)$

Matching Strip Theory to Known Vehicle Characteristics

For the example vehicles the airplane stability derivatives were known. To insure that the vehicle dynamics resulting from the strip theory calculations would agree with these known vehicle characteristics, the magnitudes of several of the strip theory parameters were adjusted slightly. Table 2 lists the four stability derivatives that were matched, as well as the strip theory parameters that were adjusted to effect the matching.

III. Computation Logic

The basic logic for computing the dynamic effects of a vortex encounter are listed below.

1) Start with known aircraft c.g. location and attitude,
2) Select strip to be considered,
3) Define location of point on desired strip in body axis system,
4) Transform location of desired point to earth-fixed axis system,
5) Compute two-dimensional earth-referenced flow at point of interest in space due to both vortices,
6) Transform earth-referenced flow at point of interest to body axis system in aircraft.
7) Compute $\Delta\alpha$ (or $\Delta\beta$, as appropriate) on desired strip,
8) Compute ΔForce on strip (due to vortex flow),
9) Repeat 2 through 8 for each strip,
10) Sum the forces and forces × lever arms for each strip to get forces and moments on aircraft due to vortex flow,
11) Add forces and moments due to vortices to forces and moments due to aircraft attitude and velocity (obtained via nondimensional stability derivatives), giving total forces and moments on aircraft,
12) Integrate aircraft equations of motion over small Δt to obtain new c.g. location and attitude,
13) Repeat 1 through 12 until desired time of flight is reached, and
14) Store results and then plot.

IV. Simulation Features

The salient features of the computer simulation are listed in Table 3.

V. Aircraft and Test Conditions

Example vortex wake encounters were simulated for two classes of aircraft: a 3200 pound, twin-engine general aviation airplane (PA-30) penetrating the vortex wake of a 30,000 pound executive jet transport (Jetstar); and a 126,000 pound commercial jet transport (CV-880) penetrating the vortex wake of a 580,000 pound jet transport (C-5A). For the PA-30, 3 and 10 mile separations were used, while for the CV-880 a 3 mile separation was simulated. These aircraft were selected because the aerodynamic data were readily available to the investigators.

Table 3 Salient features of the computer simulation

- 6-degree-of-freedom nonlinear digital simulation
- Arbitrary generating and penetrating airplanes
- Arbitrary initial conditions (penetration angles and position)
- Can use any vortex model desired
- No small-angle approximations for Euler angles
- Includes control surface position and rate limits
- Arbitrary control system logic
- Subroutine calculations:
  1) Vortex flow at any point
  2) Transform flow into body axes
  3) Compute force on each strip via strip theory
  4) Sum individual forces and forces × lever arms
  5) Numerical integration of equations of motion

Digital simulations were calculated for penetrations both normal and parallel (approximately) to the vortex wake axes. Only the roughly parallel penetrations will be discussed here because these were the most serious encounters considered. For these glancing encounters the primary measure of the severity of an upset is the maximum bank angle during the upset.

Two types of glancing encounters were considered—a glancing entry into the side of one vortex (from "outside" the vortex pair), and a glancing entry into the bottom of one vortex. These differed in one significant aspect. The side entry first produced roll in one direction (as the vortex was approached), and then suddenly rolled the vehicle over in the opposite direction (as the center of the vortex was encountered). The entry from below produced roll in one direction only. For the particular control systems used, and the entry conditions tried, larger bank angles were obtained with the entries from below. Therefore, all of the various comparisons made were based on results for entries from below.

All the simulated penetrations, with and without the control systems, were made with no pilot control action. The comparisons are made between the situation in which no action is taken to arrest the upset and that in which the control system is attempting to arrest the upset. A better comparison would include the action of the pilot-in-the-loop but that was not possible within the scope of this study. It will be considered in a follow-on study.

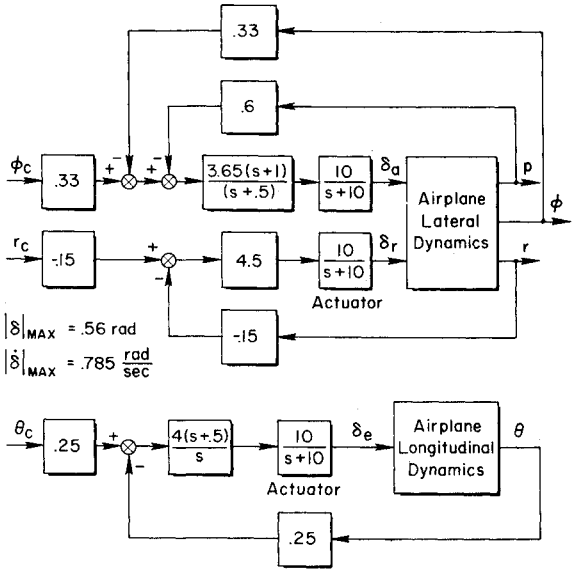

Fig. 4 Bank angle command system for PA-30.

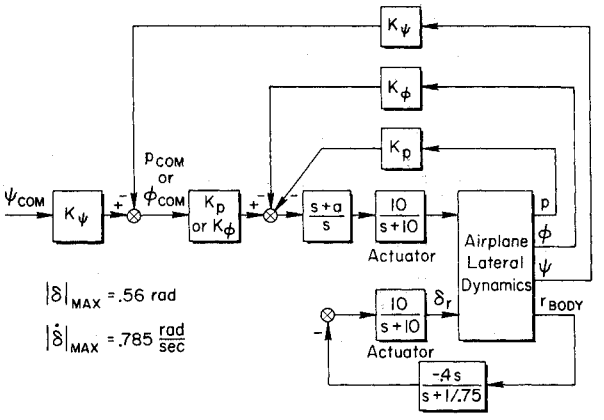

Roll Rate Command System	Bank Angle Command System	Heading Command System
K_p = .25	K_p = 2.0	K_p = 2.0
K_ϕ = 0	K_ϕ = 3.4	K_ϕ = 3.4
a = 4.0	a = .01	a = .01
K_ψ = 0	K_ψ = 0	K_ψ = 2.818

Fig. 5a Lateral block diagram for CV-880 control system.

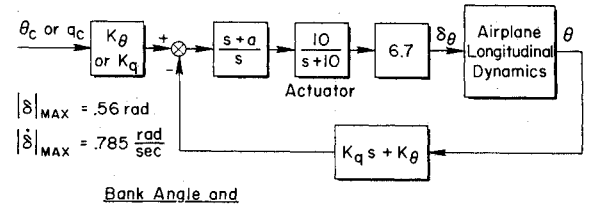

Bank Angle and Heading Command Systems	Roll Rate Command System
K_q = -.5	K_q = -.4
K_θ = .95	K_θ = 0
a = .6	a = 2.5

Fig. 5b Longitudinal block diagram for CV-880 control systems.

VI. Control Systems Description

Two different approaches were taken in defining control systems to use in the simulation tests for the PA-30 and the CV-880. Command augmentation systems had been designed and flight tested in a PA-30 aircraft at the NASA Flight Research Center.[5] Those systems were used as a starting point and modified primarily by increasing rate feedback gains for this study. The resulting systems are shown in Fig. 4.

New command augmentation systems were designed in this study for the CV-880. Figures 5a and 5b present composite lateral and longitudinal block diagrams for the control systems used with the CV-880 (i.e., rate command, attitude command, and heading command systems).

Because of the relatively low aileron control power available for the PA-30 (compared to the vortex strength used) full aileron was required to minimize the bank angle during an upset. The proper control strategy thus resembled that of a bang-bang system until the bank angle and roll rate were both relatively small. However, a bang-bang aileron position could not be achieved because of the low rate limit used for the aileron actuator. This resulted in a lag between the commanded aileron and the actual aileron position. To compensate for this lag the roll rate gain was increased to a value that would typically be considered as higher than normal. The identification of such an "abnormal" system characteristic as being desirable for minimizing vortex upsets was one of the goals of the study.

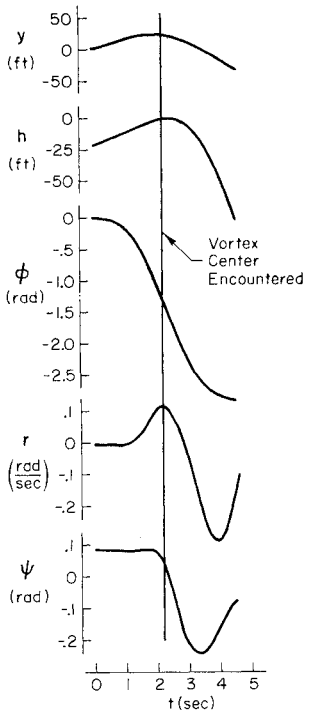

Fig. 6 PA-30 bare airplane; 3 mile separation.

VII. Results and Discussion

Calculated Time Responses

Five example vortex encounters for a 3 mile separation are presented to show the details of the upsets with and without augmentation systems. Figures 6 and 7 show the PA-30 and CV-880 without augmentation systems. Figure 8 shows a PA-30 with a bank angle command system. Figures 9 and 10 then show a CV-880 with heading command, and bank angle command systems, respectively. The roll rate command systems are not shown because they were not very effective in alleviating the upsets.

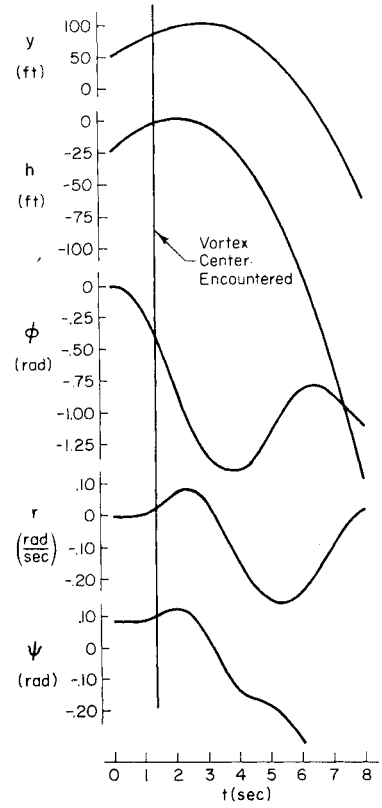

Fig. 7 CV-880 bare airplane; 3 mile separation.

Figure 6 shows that the PA-30 rolls inverted when no control is applied. It also shows that the peak yaw rate occurs at about the time the vortex center is reached. However, the interesting aspect of the peak yaw rate is the direction of yawing. The vortex is rolling the airplane to the left, but yawing it to the right. Thus, the encounter produces an uncoordinated situation wherein the motion cues could be confusing to a pilot.

Figure 7 shows the CV-880 response to a vortex encounter when no control is applied. It is qualitatively similar to the PA-30, including the uncoordinated yawing, but the maximum bank angle is less.

Figure 8 shows that for the PA-30 with a bank angle command system the aileron position limit is reached prior to encountering the center of the vortex. The bank angle trace shows the airplane rolling over to about 60° in 2½ sec, and then rolling back to wing level in another 2 sec. Notice that even though the aileron position and rate limits were reached, roll control is quite good once the central region of the vortex is passed.

Figure 9 shows an interesting point to be considered with regard to the useful control system feedback variables. In this situation the CV-880 has a heading feedback as well as a bank angle feedback to the aileron. Due to the large adverse yaw the aileron command due to heading subtracts from the aileron command due to bank angle. (The traces show ψ and φ to be very similar, but with opposite signs.) Thus, the net aileron command is quite small even though the bank angle is about 35°. This is not a good situation. During a vortex upset the control of bank angle is more important than maintaining a given heading. In fact, better heading control will ultimately be realized if good bank angle control is achieved. The conclusion to be drawn here is that a straight heading feedback is detrimental to good bank angle control.

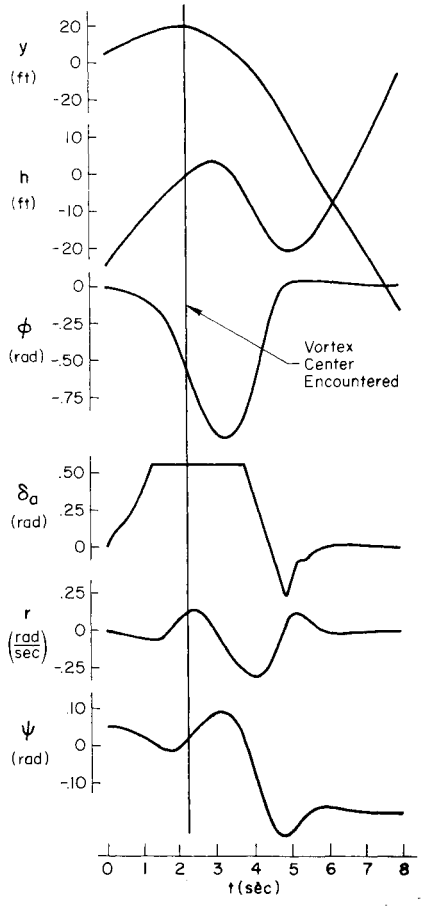

Fig. 8 PA-30 bank angle command system; 3 mile separation.

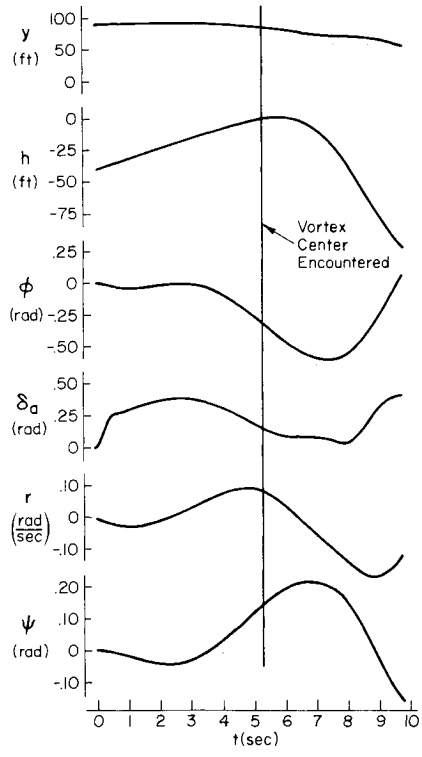

Fig. 9 CV-880 heading command system; 3 mile separation.

Figure 10 shows the traces for a control system that is the same as that used in Fig. 9, except for the removal of the heading feedback. This system is called a bank angle command system. Here it is readily seen that the bank angle never builds up, and the maximum heading change is actually about the same as that found using the heading command system! This is clearly a better system for controlling vortex wake upsets.

VIII. Summary of Results

The lateral situation was found to be more critical than the longitudinal situation, and more amenable to alleviation of vortex response via automatic control systems. The key performance metric for evaluating the upsets is the maximum bank angle experienced. Tables 4 and 5 present maximum bank angle comparisons for several types of control systems on the two example aircraft considered.

As can be seen in the comparisons in Tables 4 and 5, the automatic control systems provide a significant reduction in the maximum bank angle experienced in a vortex wake upset for both types of aircraft. However, the control systems used were specifically designed to counteract the effects of a vortex encounter, and their acceptability for suppressing motions due to random turbulence (for example) or for improving handling qualities has not been investigated.

IX. Follow-On Study

The preliminary study reported here was only intended to give a first-order assessment of the feasibility of using automatic control systems for alleviating vortex wake encounter upsets. Having shown the feasibility of such systems, a follow-on study is currently under way to answer some of the questions not addressed in the initial study. This contemplated work will include the addition of human pilot models so that comparisons can be made between a manually controlled bare airplane and a manually controlled augmented airplane, as well as between manual and automatic control during vortex encounters. The consequences of using a different vortex model will also be investigated, as will the abovementioned issue of the acceptability of a vortex alleviating system from handling qualities and gust regulation points of view.

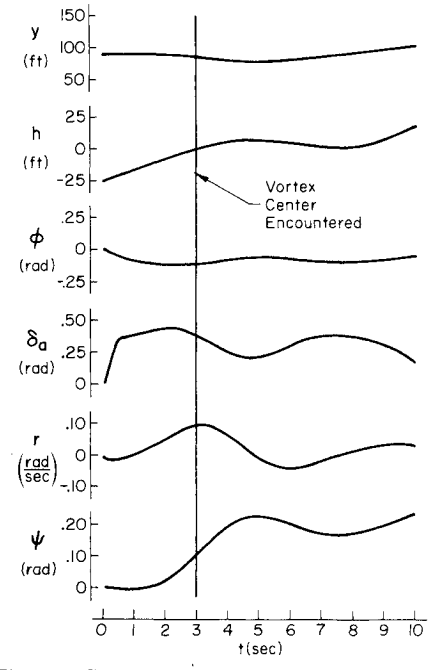

Fig. 10 CV-880 bank angle command system; 3 mile separation.

Table 4 General aviation aircraft penetrating executive jet transport wake: maximum bank angle comparison

	Separation	
	3 Mile	10 Mile
No augmentation system	180°	105°
Bank angle command system	60°	23°

Table 5 Commercial jet transport penetrating jumbo jet transport wake: maximum bank angle comparison (3 mile separation)

No augmentation system	90°
Heading command system	35°
Bank angle command system	7°
Roll rate command system	25°

X. Conclusions

As a result of a preliminary study of the effectiveness of automatic control systems in alleviating vortex wake upsets, the following conclusions were reached:

1) Specifically designed attitude command augmentation systems can provide significant alleviation of vortex wake upsets.

2) A rate damper or rate command system alone does not significantly alleviate the upsets.

3) A good vortex upset alleviating system has a higher roll rate gain than a conventional SAS.

4) A heading to aileron loop is detrimental.

5) High authority and high surface rate limits are needed for a good vortex upset alleviating system.

6) Control surface rate and position saturation effects are important particularly when a small airplane is fol-

lowing a larger one; however, significant alleviation is still possible with some saturation.

It must be emphasized that these conclusions are only meant to indicate a first-order feasibility. Further study is necessary to assess the effect of pilot action and the acceptability of this type of vortex upset alleviation system from a normal handling qualities viewpoint.

References

[1]Nelson, R. C. and McCormick, B. W., "Aircraft-Vortex Penetration," SAE Paper 730296, Wichita, Kan., 1973.

[2]Andrews, W. H., Robinson, G. H., and Larson, R. R., "Exploratory Flight Investigation of Aircraft Response to the Wing Vortex Wake Generated by Jet Transport Aircraft," NASA TN D-6655, March 1972.

[3] Robinson, G. H. and Larson, R. R., "A Flight Evaluation of Methods for Predicting Vortex Wake Effects on Trailing Aircraft," NASA TN D-6904, Nov. 1972.

[4]Von Mises, R., *Theory of Flight*, Dover, New York, 1959.

[5]Loschke, P. C., Barber, M. R., Jarvis, C. R., and Enevoldson, E. K., "Flight Evaluations of the Effect of Advanced Control Systems and Displays on the Handling Qualities of a General Aviation Airplane," SAE Paper 720316, Wichita, Kan., March 1972.

MARCH 1974 J. AIRCRAFT VOL. 11, NO. 3

Reduction of TACV Power Requirements by Multiple-Stage Air Cushions

William R. Eberle*
Purdue University, Lafayette, Ind.

One of the problems associated with tracked air cushion vehicles is their high power requirement. This paper shows that the power required for levitation for such vehicles can be significantly reduced by the use of multiple stage air cushions. A mathematical model for these air cushions is developed, and the air cushion pressures obtained from the model are compared with experimental pressures. It is shown that one of the most significant features of multiple stage air cushions is their inherent roll stability as opposed to an inherent instability for conventional air cushion designs. This inherent roll stability allows a significant reduction in the power required for levitation for tracked air cushion vehicles.

Introduction

ONE of the promising solutions for the high speed transportation requirements of the United States is the tracked air cushion vehicle. Such vehicles are capable of top speeds of 150 mph to 400 mph and, therefore, represent a significant potential increase in the speed of ground transportation vehicles. Historically, the concept of tracked air cushion vehicles has been derived from many experimental ground effects machines of the late 1950's and the 1960's. In general, these ground effects machines were designed for transportation over water or over unimproved terrain. Therefore, the designer had no control over the shape of the surface over which the vehicle operated. However, for the tracked air cushion vehicle, the vehicle travels on a track which is specifically designed for such purposes. Therefore, it is expedient to explore techniques by which the designer may reduce the power required for levitation of tracked air cushion vehicles by proper track design. This paper describes one promising method of reducing the levitation power for tracked air cushion vehicles.

The proposed method of achieving a power reduction is to provide for several stages, each of which has a peripheral jet. The resulting pressure differentials across all of the Stages provide a net lift which is greater than would be achieved by one peripheral jet. The research reported in this paper has included both analytical and experimental investigations of this concept.

Received May 2, 1973; revision received December 27, 1973. This research was supported by National Science Foundation under Grant GK-2773.

Index category: Ground (or Water-Surface) Effect Machines.

*Assistant Professor.

Figure 1 shows a cross section of a two-stage air cushion for which the air from the first stage peripheral jet is deflected into the second stage by a ramp which is part of the guideway. This ramp allows the use of two jets in series on the underside of the air cushion and results in an air cushion pressure which is greater than that obtainable for a similar flow rate with a single stage. Although other recirculation and multiple stage concepts have previously appeared in the literature,[1-3] this concept is the first to take advantage of the designer's freedom to design the track as well as the air cushion.

Analytical Model for Multiple-Stage Air Cushions

A diagram for a two-stage peripheral jet air cushion is shown in Fig. 1. The geometrical parameters associated with a two-stage air cushion are defined in Fig. 1. The first stage is like a conventional peripheral jet for which the pressure under the air cushion is maintained by the change in momentum of the jet from inward-directed to outward-directed.

Although a multiple-stage air cushion contains elements of a conventional air cushion, the analysis is more complex for the multiple-stage air cushion because of the possibility of flow beneath the outer stages. As shown in Fig. 1, the analytical model allows for air flow in both the upper and lower channels.

Air flow through the channels was assumed to be one-dimensional. This allowed rapid calculation of performance for a wide range of geometric parameters. The analytical model was used to calculate the properties of the air at stations r, c, σ, l, and n. Equations which relate the fluid properties at each of the five stations are

$$\dot{m} = \rho A V \tag{1}$$